

Parallel Spectroscopic Method for Examining Dynamic Phenomena on the Millisecond Time Scale

Christopher M. Snively,^{*,†} D. Bruce Chase,[‡] and John F. Rabolt[†]

Department of Materials Science and Engineering, University of Delaware, Newark, Delaware 19716, and DuPont Inc. Corporate Research and Development, Wilmington, Delaware 19880

Received August 22, 2008

An infrared spectroscopic technique based on planar array infrared (PAIR) spectroscopy has been developed that allows the acquisition of spectra from multiple samples simultaneously. Using this technique, it is possible to acquire spectra over a spectral range of 950–1900 cm^{-1} with a temporal resolution of 2.2 ms. The performance of this system was demonstrated by determining the shear-induced orientational response of several low molecular weight liquid crystals. Five different liquid crystals were examined in combination with five different alignment layers, and both primary and secondary screens were demonstrated. Implementation of this high-throughput PAIR technique resulted in a reduction in acquisition time as compared to both step-scan and ultra-rapid-scanning FTIR spectroscopy.

Introduction

Many phenomena of interest in materials science occur over a range of timescales spanning milliseconds to seconds. Most spectroscopic techniques are capable of either analyzing multiple samples simultaneously *or* providing high temporal resolution. However, there are several techniques that combine these two abilities, including fluorescence¹ and photoluminescence spectroscopies.²

Vibrational spectroscopic techniques are of particular interest because of the broad applicability of vibrational spectroscopic measurements to the entire spectrum of organic and inorganic materials. Fourier transform infrared (FTIR) imaging in particular has been applied as a high-throughput technique for the characterization and reaction monitoring of bead-supported organic materials,^{3,4} heterogeneous catalysts,^{3,5,6} and pharmaceuticals.⁷ FTIR imaging employs a focal plane array (FPA) detector, which provides two-dimensional spatial resolution that is utilized as a means to acquire spectra from multiple samples simultaneously. The use of an array detector lends to the advantage of scalability, such that the sample throughput is directly proportional to the number of samples that can be imaged onto the FPA detector simultaneously. One disadvantage of FTIR imaging is that the temporal resolution is limited to approximately one imaging data set per second. This has been improved upon by an approach that combines FPA detection with the time-resolved step-scan data collection scheme.⁸

Planar array infrared (PAIR) spectroscopy also employs an FPA detector. However, instead of using interferometry to encode different spectral frequencies into an interferogram, PAIR uses a spectrograph based either on a prism⁹ or a grating¹⁰ to directly image the dispersed single beam spectra

onto the FPA. The instrumental setup of a typical grating-based PAIR instrument is shown in Figure 1. PAIR is unique among infrared spectroscopic techniques in that one dimension of the FPA (the one in the plane of the figure) is used for the acquisition of spectral information, while the other (the one along the slit, out of the plane of the figure) can be used for the acquisition of spatially resolved information. Therefore, a single data set, which can be collected in a matter of seconds, contains a wealth of information that can be used in a variety of ways. In most PAIR studies, one sample is placed in front of the slit, and the data along the slit dimension are averaged to increase the signal-to-noise ratio of the data. Another approach is to split the infrared beam into two parts and image them separately onto the slit. This is useful for the simultaneous acquisition of sample and background spectra for real-time background correction or for the simultaneous acquisition of orthogonally polarized spectra for the characterization of orientation.¹¹

PAIR has been employed for the study of both static^{12,13} and dynamic¹⁴ systems. The main advantage of PAIR in the study of dynamic systems is its ability to acquire broadband spectra with submillisecond temporal resolution in a single acquisition, similar to ultrarapid-scanning FTIR.¹⁵ Thus, spectra can be acquired from dynamic systems without the need to repeat the phenomenon under study several hundreds

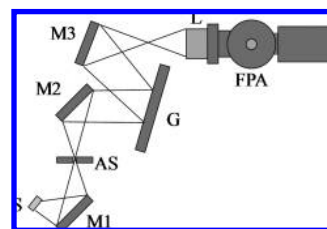


Figure 1. Schematic of PAIR instrumental setup. S is a global source, M1 is an off-axis mirror, AS is an adjustable slit, M2 and M3 are spherical mirrors, G is a plane grating, L is an adjustable focus lens, and FPA is the focal plane array detector.

* To whom correspondence should be addressed. E-mail: snively@udel.edu.

[†] University of Delaware.

[‡] DuPont Inc. Corporate Research and Development.

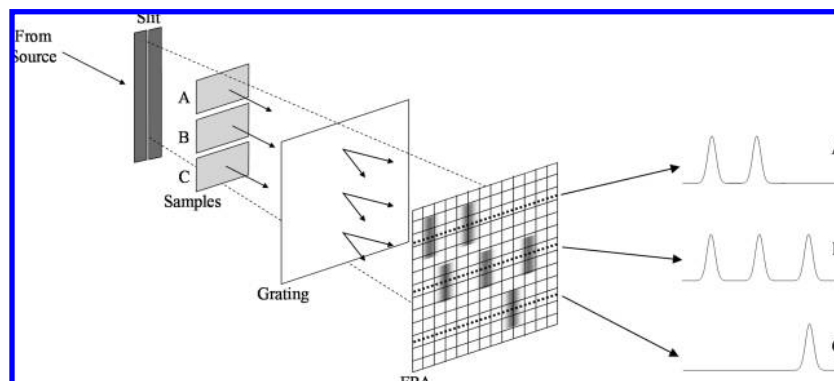


Figure 2. High-throughput PAIR schematic. After the light from the source passes through the slit and the samples, it is dispersed by the grating and imaged onto the FPA. Thus, a single image captured by the FPA contains spectral information from multiple samples.

or thousands of times, as is required with step-scan FTIR,^{8,16} asynchronous FTIR,¹⁷ or single-channel dispersive approaches.¹⁸

This work extends this concept to the acquisition of spectra from multiple samples simultaneously. Instead of using the slit dimension for the acquisition of information from different regions of a single sample, several samples are placed along the slit dimension, and spectral information is acquired from them simultaneously in a single experiment. The basic concept behind this approach is illustrated schematically in Figure 2. Similar to FTIR imaging, the PAIR approach to high-throughput sampling also benefits from a multiple-sample multiplex advantage, in that the sample throughput increases in direct proportion to the number of samples that are placed in the field of view of the instrument. Thus, by proper design of samples, sampling accessories, and associated optics, any number of samples up to the number of pixel rows along the slit dimension can be analyzed simultaneously.

As an example system, the response of a nematic liquid crystal to an applied shear strain was used. The combination of vibrational spectroscopy with shear perturbation has been discussed briefly in the literature,^{19–21} and was shown to have a similar effect as the application of an electric field. The ability to collect the same type of information in a parallel high-throughput manner would be useful because it would allow the rapid study of many different liquid crystal formulations in combination with a variety of alignment layers.

Experimental Section

Boron-doped silicon wafers with resistivity greater than $20 \Omega \text{ cm}^{-1}$ (Virginia Semiconductor, Inc.) were employed as substrates for all experiments. Room-temperature single-component nematic liquid crystal 4-*n*-pentyl-4'-cyanobiphenyl (5CB) and nematic mixture E7 (which is composed predominantly of 5CB) were obtained from Merck. Lecithin was obtained from Alfa Aesar, while 4-*n*-heptyl-4'-biphenylcarboxylic acid (c7CB) was synthesized according to literature procedures. All other materials were obtained from Aldrich. All wafers were cleaned using piranha solution (50:50 mixture of sulfuric acid and hydrogen peroxide) before surface treatments were applied. Poly(caprolactone) and poly(vinyl alcohol) layers were prepared by spin coating

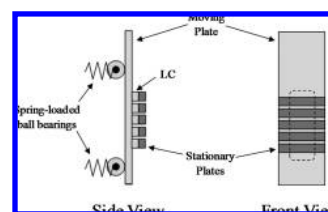


Figure 3. Schematic of the sample arrangement used to measure the effects of shear on five LC samples simultaneously. The stationary plates are attached to a metal plate that is not shown for clarity. The dashed line in the front view represents the opening in this metal plate, through which the IR beam passes.

from dilute solution. Aminopropyltriethoxysilane (γ -APS) and octadecyltrichlorosilane (ODTS) monolayers were prepared from dilute toluene solutions. Lecithin was applied from dilute hexane solution using a cotton applicator. The deposition of the lecithin and polymer films was evident from the presence of interference colors, whereas the presence of the monolayers was verified via water contact angle.

A PAIR instrument similar to those previously reported²² was utilized and consisted of a Czerny–Turner spectrograph employing a 50 groove/mm grating and $500 \mu\text{m}$ wide slit. A 128×128 -pixel HgCdTe FPA detector (Santa Barbara Focal Plane) operating in the snapshot mode²³ at a frame rate of 460 Hz and an integration time of $120 \mu\text{s}$ was employed for detection. A $5.5 \mu\text{m}$ long pass filter was included to eliminate contributions from beyond the first diffraction order. With this setup, it is possible to collect spectra over the $950\text{--}1900 \text{ cm}^{-1}$ spectral range with a temporal resolution of 2.2 ms. All data processing steps, including dark background subtraction, absorbance calculation, and coaddition, were performed using custom routines written in Matlab. Baseline correction and data extraction was performed in Grams (Thermo Galactic).

Sample modulation was carried out using a Polymer Stretcher (Manning Applied Technologies) that was modified to work in the shear geometry with multiple samples, as illustrated schematically in Figure 3. A metal plate was fastened to one side of the Polymer Stretcher and was used to support the stationary sample substrates, which measured approximately $4 \times 30 \text{ mm}$. A larger substrate ($20 \times 50 \text{ mm}$) was attached to the moving arm of the Polymer Stretcher and used to apply the shear strain to all samples. The spacing between the plates was held constant at $15 \mu\text{m}$ by the use of glass rod spacers and gentle pressure from spring-loaded ball

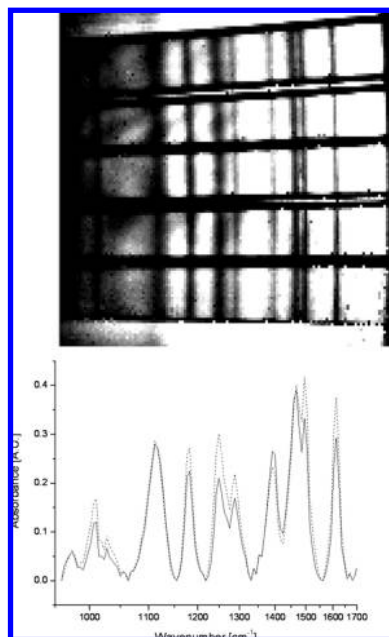


Figure 4. (top) Raw intensity image of five E7 samples. (bottom) Spectra extracted from one sample before (solid line) and after (dotted line) the application of step shear.

bearings. The samples were perturbed by feeding the output of a DS345 arbitrary waveform generator (Stanford Research Systems) into the Polymer Stretcher electronic controller. A second waveform generator was employed as a pulse generator to synchronize the data collection and sample perturbation. The extent of shear was quantified by direct readout from the Polymer Stretcher electronics and was calibrated using a microscope equipped with a stage micrometer.

The samples were prepared such that the common plate of the sample sandwich was coated with lecithin, while the smaller plates were coated with one of the aligning layers. The lecithin served to induce homeotropic alignment,²⁴ in which the long axes of the molecules are aligned perpendicular to the substrates. Therefore, when shear is applied, the long axes of the molecules align along the shear direction, leading to an increase in measured absorbance for bands that have transition moments aligned parallel to the long axis. Likewise, a decrease in intensity is observed for bands that have transition moments aligned perpendicular to the long axis.²¹ The thermal histories of the samples were normalized by heating them above the nematic to isotropic transition temperature and allowing them to cool to room temperature before the shear experiments were performed. In a single experiment, it was possible to examine the response of a single LC with five different alignment layers: PVOH, PCL, γ -APS, ODTs, and the native oxide layer of the Si wafer.

Results and Discussion

An example of the type of data that can be acquired using the above setup is shown in Figure 4. The image was generated by plotting the raw output from the FPA and illustrates that all five samples and their spectra can be viewed simultaneously. Each sample appears as a horizontal strip, with absorption bands appearing as dark vertical lines.

Image curvature, resulting from the use of off-axis optical elements, can be seen in the image. Unlike in previous investigations,¹¹ no attempt was made to correct for this curvature. Although successive rows were coadded to increase the signal-to-noise ratio (SNR) of the data, no effect of image curvature on spectral resolution was observed because the coaddition was carried out over short vertical segments of the image. Differences in the frequency axis between samples caused by this curvature were accounted for by calibrating each image segment separately.

The spectra shown at the bottom of Figure 4 are the result of the coaddition of spectra from the sample at the top of the image. The spectra were extracted immediately before and after the application of a 100 μm shear step. It is known that 5CB exhibits flow-aligning behavior,²⁵ in which the nematic director tips in the direction of an applied shear force. An increase in most of the bands is expected, and indeed observed, since most of the vibrational modes in this spectral region have a transition moment vector that is aligned parallel to the long axis of the molecule.²⁶ One exception is the CH chain deformation mode at 1400 cm^{-1} , which is aligned perpendicular to the long axis of the molecule. In this way, the tilt angle of the LC can be directly observed as a change in relative absorbance intensity.

The dynamic response of 5CB to a shear strain step was examined in detail in a previous publication²¹ and was seen to have a similar appearance as when an electric field pulse was applied. The general shape of the time dependent behavior exhibits an initial sudden change in absorbance intensity, followed by a slower relaxation back to the initial state. This response is governed by the strength of the interaction between the LC and the alignment layers applied to the substrates.

Time resolved high throughput PAIR spectroscopy can be employed as both a primary and secondary screening tool, as illustrated here with the example of determining the dynamic response of several liquid crystal and alignment layer combinations. Five different liquid crystals were examined: 5CB, E7, and 5CB doped with 0.5% w/w of three different additives. Five different alignment layers were also employed: silicon with a native oxide layer, ODTs, and γ -APS monolayers and PCL and PVOH spun-on films.

The primary screen was set up as a matrix of 25 experiments, where each LC/alignment layer combination was examined under the influence of a single shear step. This was accomplished using a total of five experiments, with five samples being analyzed simultaneously. In each experiment, a single LC was examined under the influence of five different alignment layers. The results of this primary screen are summarized in Figure 5, which shows the dynamic response of the 1610 cm^{-1} C=C phenyl ring stretching mode for all 25 experiments. These results show a variety of different responses to the perturbation, including differing amounts of absorbance change and different rates of relaxation back to equilibrium.

As an example of a secondary screen, two samples were chosen from the original primary screening experiment, and a more detailed study was carried out. The samples chosen were E7 with ODTs and native oxide (SiO_2) surfaces. The

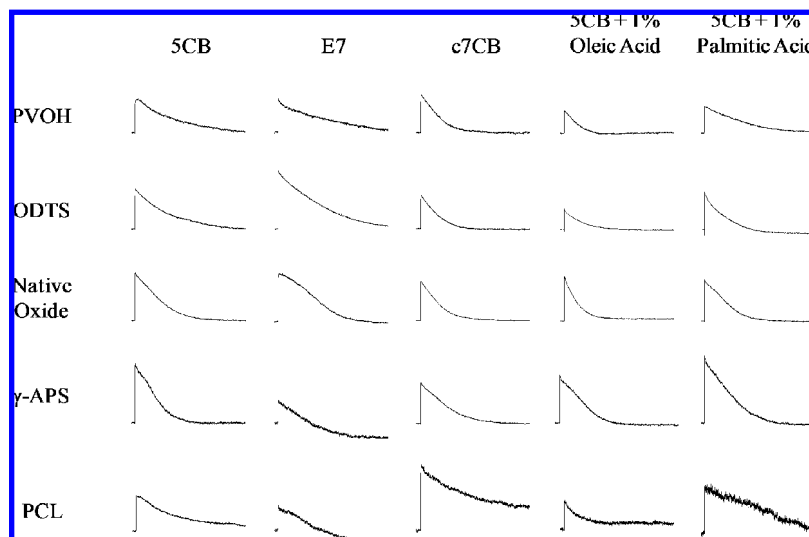


Figure 5. Dynamic response curves obtained by plotting the 1610 cm^{-1} band as a function of time during the primary screen of 25 different LC samples. The scale of each graph is the same, with the y-axis spanning from 0 to 0.2 absorbance units and the x-axis spanning from 0 to 3.25 s.

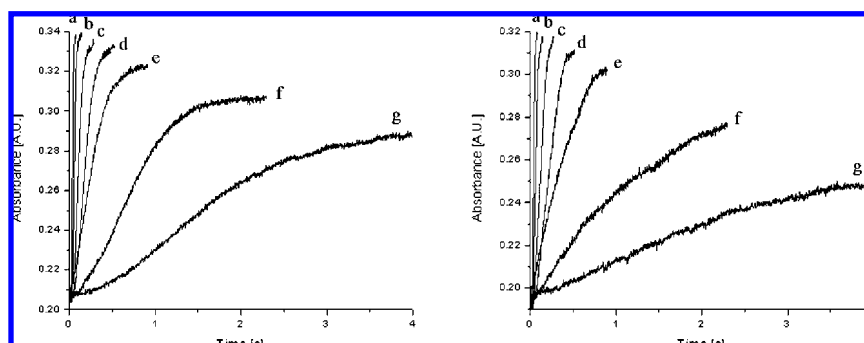


Figure 6. Secondary screening results from (left) E7/ODTS and (right) E7/native oxide, obtained at constant shear rates of (a) 140, (b) 68, (c) 27, (d) 14, (e) 6.8 (f) 2.7, and (g) 1.4 s^{-1} . These plots were generated using the same absorption band as in Figure 5.

response of these samples to an applied shear with a constant shear rate, instead of the shear step used in the primary screen, was examined. Figure 6 shows the response of both samples to shear rates spanning 2 orders of magnitude. Even though the difference in the response of these two samples in the primary screen was subtle, more pronounced differences become apparent in the secondary screen. At lower strain rates, the ODTS sample reached a steady state tilt angle at shorter times compared to the SiO_2 sample, which implies the presence of weaker intermolecular interactions in the case of ODTS. It is known that ODTS causes cyanobiphenyl LCs to adopt a homeotropic orientation, whereas SiO_2 induces planar orientation.²⁴ This indicates that the intermolecular interactions are stronger in the case of SiO_2 , corroborating the results obtained in the secondary screening experiment. Samples of interest identified using this secondary screen can then be individually analyzed in more detail to maximize the signal-to-noise ratio (SNR) of the data.

As with all techniques, it should be noted that there are tradeoffs associated with high throughput PAIR spectroscopy. The total number of samples that can be examined simultaneously is limited by the ability to design appropriate sampling accessories, analogous to the case of FTIR imaging.²⁷ In the case of the liquid crystal experiments illustrated here, there is an upper limit of approximately 10 samples because of the limited ability to cleave and manipulate pieces

of silicon that are smaller than a few millimeters in width. In the extreme limit, the total number of samples is limited to the number of rows of pixels in the FPA. Since row coaddition is employed to increase the SNR, there is also a tradeoff between the maximum achievable SNR and the number of samples that can be analyzed simultaneously. It is possible to improve the SNR by coadding successive spectra, thereby sacrificing temporal resolution. This is possible only when the temporal response of the chemical system under study is sufficiently slow that coadding does not degrade the fidelity of the temporal information. Finally, the SNR can also be enhanced by performing the experiment multiple times and averaging the data from multiple experiments together, similar to the approach taken in step-scan FTIR, although this would only be possible with samples that do not undergo irreversible changes during perturbation.

The real advantage of high-throughput PAIR spectroscopy is realized when one considers the actual experimental time involved in data acquisition. With step-scan FTIR, a single experiment, equivalent to one of the response curves shown in Figure 5, can be completed in about 10 min, assuming that the SNR is high enough to require only a few coadditions. Using PAIR, it is possible to acquire five equivalent data sets in 3.25 s, leading to a reduction in collection time of more than 2 orders of magnitude. Data processing and workup time are approximately the same for

PAIR and FTIR. It should be mentioned, however, that step-scan FTIR still retains the advantage of being able to achieve a temporal resolution several orders of magnitude greater than PAIR. For this particular sample geometry, sample preparation contributes significantly to the overall experimental time. The use of high-throughput PAIR spectroscopy will have an additional advantage in this case because the preparation of the five samples used in these studies requires approximately the same amount of time for the preparation of one sample that would be employed in an FTIR experiment. Thus, PAIR retains an advantage in terms of collection time over techniques such as ultra-rapid-scanning FTIR,¹⁵ which have similar data collection times.

Conclusions

We have demonstrated that PAIR spectroscopy is capable of acquiring spectral information from multiple samples simultaneously with a temporal resolution on the order of milliseconds. The dynamic rheological response of liquid crystals under the influence of different alignment layers served to demonstrate the utility of this approach to probe intermolecular interactions. The real advantage of this technique is its ability to acquire information in a one-shot mode, where the phenomenon of interest needs to occur exactly once in order to be studied. This not only allows the study of irreversible phenomena, but also decreases the experimental time when compared with conventional approaches, allowing for a more rapid discovery and optimization of systems in which dynamic behavior is critical to the desired properties. This high-throughput spectroscopic method is not limited to the study of rheological behavior but is generally applicable to any dynamic phenomenon that exhibits changes in the infrared spectra. It is anticipated that high-throughput PAIR will be useful for the study of other types of dynamic phenomena in materials, as well as other areas, such as high-throughput liquid chromatography.

Acknowledgment. The authors acknowledge funding from the National Science Foundation under Grant DMR-0704970 and the National Institutes of Health under Grant 4R33EB03288-03.

References and Notes

- (1) Ma, Y. F.; Shortreed, M. R.; Yeung, E. S. *Anal. Chem.* **2000**, *72*, 4640–4645.

- (2) Atienzar, P.; Corma, A.; Garcia, H.; Serra, J. M. *Chem.—Eur. J.* **2004**, *10*, 6043–6047.
- (3) Snively, C. M.; Oskarsdottir, G.; Lauterbach, J. *J. Comb. Chem.* **2000**, *2*, 243–245.
- (4) Fenniri, H.; Terreau, O.; Chun, S. K.; Oh, S. J.; Finney, W. F.; Morris, M. D. *J. Comb. Chem.* **2006**, *8*, 192–198.
- (5) Busch, O. M.; Brijoux, W.; Thomson, S.; Schuth, F. *J. Catal.* **2004**, *222*, 174–179.
- (6) Snively, C. M.; Oskarsdottir, G.; Lauterbach, J. *Angew. Chem., Int. Ed.* **2001**, *40*, 3028–3030.
- (7) Chan, K. L. A.; Kazarian, S. G. *J. Comb. Chem.* **2005**, *7*, 185–189.
- (8) Bhargava, R.; Levin, I. W. *Appl. Spectrosc.* **2003**, *57*, 357–366.
- (9) Keltner, Z.; Kayima, K.; Lanzarotta, A.; Lavalle, L.; Canepa, M.; Dowrey, A. E.; Story, G. M.; Marcott, C.; Sommer, A. *J. Appl. Spectrosc.* **2007**, *61*, 909–915.
- (10) Elmore, D. L.; Tsao, M. W.; Frisk, S.; Chase, D. B.; Rabolt, J. F. *Appl. Spectrosc.* **2002**, *56*, 145–149.
- (11) Pelletier, I.; Pellerin, C.; Chase, D. B.; Rabolt, J. F. *Appl. Spectrosc.* **2005**, *59*, 156–163.
- (12) Elmore, D. L.; Chase, D. B.; Liu, Y. J.; Rabolt, J. F. *Vib. Spectrosc.* **2004**, *34*, 37–45.
- (13) Snively, C. M.; Kim, Y. S.; Chase, D. B.; Rabolt, J. F. *Appl. Spectrosc.* **2008**, *62*, 337–339.
- (14) Pellerin, C.; Frisk, S.; Rabolt, J. F.; Chase, D. B. *Appl. Spectrosc.* **2004**, *58*, 799–803.
- (15) Griffiths, P. R.; Hirsche, B. L.; Manning, C. J. *Vib. Spectrosc.* **1999**, *19*, 165–176.
- (16) Palmer, R. A.; Manning, C. J.; Rzepiela, J. A.; Widder, J. M.; Chao, J. L. *Appl. Spectrosc.* **1989**, *43*, 193–195.
- (17) Masutani, K.; Sugisawa, H.; Yokota, A.; Furukawa, Y.; Tasumi, M. *Appl. Spectrosc.* **1992**, *46*, 560–567.
- (18) Urano, T. I.; Hamaguchi, H. *Chem. Phys. Lett.* **1992**, *195*, 287–292.
- (19) Nakano, K. *Tribol. Lett.* **2003**, *14*, 17–24.
- (20) Soga, I.; Dhinojwala, A.; Granick, S. *Langmuir* **1998**, *14*, 1156–1161.
- (21) Snively, C. M.; Rabolt, J. F.; Chase, D. B. *Vib. Spectrosc.* in press.
- (22) Pellerin, C.; Snively, C. M.; Chase, D. B.; Rabolt, J. F. *Appl. Spectrosc.* **2004**, *58*, 639–646.
- (23) Snively, C. M.; Pellerin, C.; Rabolt, J. F.; Chase, D. B. *Anal. Chem.* **2004**, *76*, 1811–1816.
- (24) Cognard, J. *Mol. Cryst. Liq. Cryst.* **1982**, *Suppl. 1*, 1–77.
- (25) Gu, D. F.; Jamieson, A. M.; Wang, S. Q. *J. Rheol.* **1993**, *37*, 985–1001.
- (26) McFarland, C. A.; Koenig, J. L.; West, J. L. *Appl. Spectrosc.* **1993**, *47*, 598–605.
- (27) Snively, C. M.; Lauterbach, J. *Spectroscopy* **2002**, *17*, 26–33.